Eidgenössische Technische Hochschule Zürich

Ecole polytechnique fédérale de Zurich
Politecnico federale di Zurigo
Swiss Federal Institute of Technology Zurich

Modelling Micro Mass and Heat Transfer for Gases Using Extended Continuum Equations

Henning Struchtrup[†] and Manuel Torrilhon

Research Report No. 2008-13
May 2008

Seminar für Angewandte Mathematik
Eidgenössische Technische Hochschule
CH-8092 Zürich
Switzerland

[†]Dept. of Mechanical Engineering, University of Victoria, Canada / mail: struchtr@uvic.ca

Modelling Micro Mass and Heat Transfer for Gases Using Extended Continuum Equations

Henning Struchtrup[†] and Manuel Torrilhon

Seminar für Angewandte Mathematik
Eidgenössische Technische Hochschule
CH-8092 Zürich
Switzerland

Research Report No. 2008-13 May 2008

Abstract

This paper presents recent contributions to the development of macroscopic continuum transport equations for micro gas flows. Within kinetic theory of gases a combination of the Chapman-Enskog expansion and Grad's moment method yields the regularized 13 moment equations (R13 equations) which are of high approximation order. In addition, a complete set of boundary conditions can be derived from the boundary conditions of the Boltzmann equations. The R13 equations are linearly stable and their results for moderate Knudsen numbers stand in excellent agreement to DSMC simulations.

We give analytical expressions for heat and mass transfer in micro-channels. These expressions help to understand the complex interaction of fluid variables in micro-scale systems. In particular, the R13 model is capable to predict and explain the Knudsen minimum of mass flow rate in Poiseuille flows.

[†]Dept. of Mechanical Engineering, University of Victoria, Canada / mail: struchtr@uvic.ca

1 Introduction

Processes in micro-scale flows of gases or equivalently in rarefaction situations are well described by the Boltzmann equation [6] which describes the evolution of the particle distribution function in phase space, i.e. on the microscopic level.

The relevant scaling parameter to characterize processes in micro-flow gases is the Knudsen number Kn, defined as the ratio between the mean free path of a particle and a relevant length scale. If the Knudsen number is small, the Boltzmann equation can be reduced to simpler models, which allow faster solutions. Indeed, if $Kn < 0.01$ (say), the hydrodynamic equations, the laws of Navier-Stokes and Fourier (NSF), can be derived from the Boltzmann equation, e.g. by the Chapman-Enskog method [20]. The NSF equations are macroscopic equations for mass density ρ, velocity v_i and temperature T, and thus pose a mathematically less complex problem than the Boltzmann equation.

Macroscopic equations for rarefied gas flows at Knudsen numbers above 0.01 promise to replace the Boltzmann equation with simpler equations that still capture the relevant physics. The Chapman-Enskog expansion is the classical method to achieve this goal, but the resulting Burnett and super-Burnett equations are unstable [4]. To fix these problems in the framework of Chapman-Enskog expansion is cumbersome [5, 10]. Nevertheless, in some cases Burnett equations could be used for simulations of non-equilibrium gases [1, 13].

A classical alternative is Grad's moment method [8] which extends the set of variables by adding deviatoric stress tensor σ_{ij}, heat flux q_i, and possibly higher moments of the velocity distribution function (phase density) of the particles. The resulting equations are stable but lead to spurious discontinuities in shocks [34]. Nevertheless, some successes have been obtained with moment methods and popularity is raising, see [17, 2, 12, 7, 18]. However, for a given value of the Knudsen number it is not clear what set of moments one would have to consider [20].

Struchtrup and Torrilhon combined both approaches by performing a Chapman-Enskog expansion around a non-equilibrium phase density of Grad type [27, 29] which resulted in the "Regularized 13 moment equations" (R13 equations) which form a stable set of equations for the 13 variables $(\rho, v_i, T, \sigma_{ij}, q_i)$ of super-Burnett order, i.e., of third order in the Knudsen number when asymptotically expanded. The next Section gives a review of this original derivation. An alternative approach to the problem was presented by Struchtrup in [22, 24], partly based on earlier work by Müller et al. [16]. This Order-of-Magnitude-Method is based on a rigorous asymptotic analysis of the infinite hierarchy of the moment equations. A brief outline is also given in the next Section.

One of the biggest problems for all models beyond NSF is to prescribe suitable boundary conditions for the extended equations, which should follow from the boundary conditions for the Boltzmann equation. This task was recently tackled

in [9], and the general solution to the problem [30] will be discussed after the derivation of the equations, when we present boundary conditions for the R13 equations.

The second part of the paper will survey the properties of the R13 equations, which are linearly stable, obey an H-theorem for the linear case, contain the Burnett and super-Burnett equations asymptotically, predict phase speeds and damping of ultrasound waves in excellent agreement to experiments, yield smooth and accurate shock structures for all Mach numbers, and exhibit Knudsen boundary layers and the Knudsen minimum of channel flow in excellent agreement to DSMC simulations. The paper reviews detailed informations about the performance of R13 for Poiseuille flow in micro-channels and discusses how micro-variables enter and influence the classical fluid dynamical relations.

The interested reader is referred to the cited literature, including the monograph [20].

2 Derivation of R13

The derivation of the regularized 13-moment-equations has been done in two ways. Both ways give specific insight into the structure and properties of the theory.

2.1 Based on a Pseudo-Equilibrium

The original derivation [27] develops an enhanced constitutive theory for Grad's moment equations. The closure procedure of Grad is too rigid and needs to be relaxed. The new theory can be summarized in three steps

1. Identify the set of variables U and higher moments V that need a constitutive relation in Grad's theory.
2. Formulate evolution equations for the difference $R = V - V^{(\mathrm{Grad})}(U)$ of the constitutive moments and their Grad relation.
3. Perform an asymptotic expansion of R alone while fixing *all* variables U of Grad's theory.

This procedure can in principle be performed on any system obtained by Grad's moment method, i.e., any number of moments can be considered as basic set of variables. For the derivation of R13 the first 13 moments density, velocity, temperature, stress deviator and heat flux have been considered in accordance with the classical 13-moment-case of Grad.

In the classical Grad approach the difference R is considered to be zero: All constitutive moments follow from lower moments by means of Grad's distribution $V = V^{(\mathrm{Grad})}(U)$. This rigidity causes hyperbolicity but also artifacts like subshocks and poor accuracy. However, the evolution equation for R is in general not an identity. Instead it describes possible deviations of Grad's closure. The constitutive theory of R13 takes these deviations into account.

The evolution equation for R can not be solved exactly because it is influenced by even higher moments. Hence, an approximation is found by asymptotic expansion. In doing this, step 3 requires a modeling assumption about a scaling cascade of the higher order moments. In the asymptotic expansion of R we fix lower moments like density and temperature but also non-equilibrium quantities like stress and heat flux. The assumption is that the higher moments R follow a faster relaxation or bear a smaller scale of significance. The expansion can be considered as an expansion around a non-equilibrium (pseudo-equilibrium).

The result for R after one expansion step is a relation that couples R to gradients of the variables U, in R13 these are gradients of stress and heat flux. The gradient terms enter the divergences in the equations for stress and heat flux and produce dissipative second order derivatives. The final system is a regularization of Grad's 13-moment-equations. The procedure resembles the derivation of the NSF-system. Indeed the NSF equations can be considered as regularization of Euler equations (i.e., Grad's 5-moment-system).

2.2 Based on Order of Magnitude

The Order-of-Magnitude-Method [22, 24] considers the infinite system of moment equations resulting from Boltzmann's equation. It does not depend on Grad's closure relations and does not directly utilize the result of asymptotic expansions. The method finds the proper equations with order of accuracy λ_0 in the Knudsen number by the following three steps:

1. Determination of the order of magnitude λ of the moments.
2. Construction of moment set with minimum number of moments at order λ.
3. Deletion of all terms in all equations that would lead only to contributions of orders $\lambda > \lambda_0$ in the conservation laws for energy and momentum.

Step 1 is based on a Chapman-Enskog expansion where a moment φ is expanded according to $\varphi = \varphi_0 + Kn\,\varphi_1 + Kn^2\varphi_2 + ...$, and the leading order of φ is determined by inserting this ansatz into the complete set of moment equations. A moment is said to be of leading order λ if $\lambda_\beta = 0$ for all $\beta < \lambda$. This first step agrees with the ideas of [16]. Alternatively, the order of magnitude of the

moments can be found from the principle that a single term in an equation cannot be larger in size by one or several orders of magnitude than all other terms [25].

In Step 2, new variables are introduced by linear combination of the moments originally chosen. The new variables are constructed such that the number of moments at a given order λ is minimal. This step gives an unambiguous set of moments at order λ.

Step 3 follows from the definition of the order of accuracy λ_0: A set of equations is said to be accurate of order λ_0, when stress and heat flux are known within the order $\mathcal{O}\left(Kn^0\right)$.

The order of magnitude method gives the Euler and NSF equations at zeroth and first order, and thus agrees with the Chapman-Enskog method in the lower orders [22]. The second order equations turn out to be Grad's 13 moment equations for Maxwell molecules [22], and a generalization of these for molecules that interact with power potentials [20, 24]. At third order, the method was only performed for Maxwell molecules, where it yields the R13 equations [22]. It follows that R13 satisfies some optimality when processes are to be described with third order accuracy.

2.3 Result

Here, we display the original R13 equations from [27] which are build from the general conservation laws for a monatomic gas with mass density ρ, velocity v_i, and the temperature θ in energy units,

$$\frac{\partial \varrho}{\partial t} + \frac{\partial \varrho v_k}{\partial x_k} = 0, \tag{1}$$

$$\varrho \frac{\partial v_i}{\partial t} + \varrho v_k \frac{\partial v_i}{\partial x_k} + \frac{\partial p}{\partial x_i} + \frac{\partial \sigma_{ik}}{\partial x_k} = 0 \tag{2}$$

$$\frac{3}{2}\varrho \frac{\partial \theta}{\partial t} + \frac{3}{2}\varrho v_k \frac{\partial \theta}{\partial x_k} + \frac{\partial q_k}{\partial x_k} + \left(p\delta_{ij} + \sigma_{ij}\right)\frac{\partial v_i}{\partial x_j} = 0 \tag{3}$$

where δ_{ij} is the Kronecker symbol or identity matrix. For the pressure p we assume the ideal gas law $p = \rho\,\theta$. We use Cartesian index notation with $i, j, k, l \in \{1, 2, 3\}$ and summation convention. The additional evolution equations that closes the system are given by

$$\frac{\partial \sigma_{ij}}{\partial t} + \frac{\partial \sigma_{ij} v_k}{\partial x_k} + \frac{4}{5}\frac{\partial q_{\langle i}}{\partial x_{j\rangle}} + 2p\frac{\partial v_{\langle i}}{\partial x_{j\rangle}} + 2\sigma_{k\langle i}\frac{\partial v_{j\rangle}}{\partial x_k} + \frac{\partial m_{ijk}}{\partial x_k} = -\frac{p}{\mu}\sigma_{ij} \tag{4}$$

for the stress deviator σ_{ij} and

$$\frac{\partial q_i}{\partial t} + \frac{\partial q_i v_k}{\partial x_k} + p\frac{\partial(\sigma_{ik}/\rho)}{\partial x_k} + \frac{5}{2}(p\delta_{ik}+\sigma_{ik})\frac{\partial \theta}{\partial x_k} - \frac{\sigma_{ij}}{\varrho}\frac{\partial \sigma_{jk}}{\partial x_k} + (m_{ijk} + \frac{6}{5}q_{(i}\delta_{jk)} + q_k\delta_{ij})\frac{\partial v_j}{\partial x_k} + \frac{1}{2}\frac{\partial \hat{R}_{ik}}{\partial x_k} = -\frac{2p}{3\mu}q_i \quad (5)$$

the heat flux q_i with μ the viscosity of the gas. Round brackets give the symmetric part of a tensor, while angular brackets around indices denote the symmetric deviatoric part, e.g., $A_{\langle ij\rangle} = A_{(ij)} - \frac{1}{3}A_{kk}\delta_{ij} = \frac{1}{2}(A_{ij}+A_{ji}) - \frac{1}{3}A_{kk}\delta_{ij}$ and analogously for three indices, see [20].

Note, that these equations include the classical laws of Navier-Stokes and Fourier for stress deviator and heat flux. They can be formally recovered by setting σ_{ij}, q_i, m_{ijk} and $\hat{R}_{ij}$ to zero on the left hand side only. The additional terms in the equations beyond the classical laws allow for inertial effects and non-gradient transport. That is, stress and heat flux are not anymore slaved to the thermodynamic fluxes, velocity gradient and temperature gradient.

The remaining quantities m_{ijk} and $\hat{R}_{ij}$ represent higher moments and as such they form fluxes of stress and heat flux. These are zero in the Grad case, but the R13 theory provides the gradient expressions

$$m_{ijk} = -2\mu\,\frac{\partial(\sigma_{\langle ij}/\rho)}{\partial x_{k\rangle}} + \frac{8}{10p}q_{\langle i}\sigma^{(\mathrm{NSF})}_{jk\rangle}\,, \quad (6)$$

$$R_{ij} = -\frac{24}{5}\mu\,\frac{\partial(q_{\langle j}/\rho)}{\partial x_{j\rangle}} + \frac{32}{25p}q_{\langle i}q^{(\mathrm{NSF})}_{j\rangle} + \frac{24}{7\rho}\sigma_{k\langle i}\sigma^{(\mathrm{NSF})}_{j\rangle k}\,, \quad (7)$$

$$R = -12\mu\,\frac{\partial(q_k/\rho)}{\partial x_k} + \frac{8}{p}q_k q^{(\mathrm{NSF})}_k + \frac{6}{\rho}\sigma_{ij}\sigma^{(\mathrm{NSF})}_{ij}\,. \quad (8)$$

with $\hat{R}_{ij} = R_{ij} + \frac{1}{3}R\delta_{ij}$ and the abbreviations

$$\sigma^{(\mathrm{NSF})}_{ij} = -2\mu\,\frac{\partial v_{\langle i}}{\partial x_{j\rangle}}, \qquad q^{(\mathrm{NSF})}_i = -\frac{15}{4}\mu\,\frac{\partial \theta}{\partial x_i}. \quad (9)$$

In total the R13 system is given by non-linear parabolic-hyperbolic partial differential equations with relaxation. In that sense it resembles the mathematical structure of the NSF equations.

3 Boundary Conditions for R13

The computation of boundary conditions for the R13 equations is based on Maxwell's model for boundary conditions for the Boltzmann equation [6, 20, 14], which

states that a fraction χ of the particles hitting the wall is thermalized, while the remaining $1-\chi$ particles are specularly reflected. Boundary conditions for moments follow by taking moments of the boundary conditions of the Boltzmann equation. To produce meaningful boundary conditions, one needs to obey the following rules:

1. *Continuity*: In order to have meaningful boundary conditions for all accommodation coefficients $\chi \in [0, 1]$, only boundary conditions for tensors with an odd number of normal components should be considered [9].

2. *Consistency*: Only boundary conditions for fluxes that actually appear in the equations should be considered [30].

3. *Coherence*: The same number of boundary conditions should be prescribed for the linearized and the non-linear equations [30].

The application of Rules 1 and 2 is straight forward and yields the following set of kinetic boundary conditions (t and n denote tangential and normal tensor components, respectively) for moments

$$\begin{aligned}
\sigma_{tn} &= -\beta\left(P\,V_t + \tfrac{1}{2}m_{tnn} + \tfrac{1}{5}q_t\right)\\
q_n &= -\beta\left(2P\,\Delta\theta + \tfrac{5}{28}R_{nn} + \tfrac{1}{15}R + \tfrac{1}{2}\theta\,\sigma_{nn} - \tfrac{1}{2}P\,V_t^2\right)\\
R_{tn} &= \beta\left(P\,\theta\,V_t - \tfrac{1}{2}\theta\,m_{tnn} - \tfrac{11}{5}\theta\,q_t - P\,V_t^3 + 6P\,\Delta\theta V_t\right)\\
m_{nnn} &= \beta\left(\tfrac{2}{5}P\,\Delta\theta - \tfrac{1}{14}R_{nn} + \tfrac{1}{75}R - \tfrac{7}{5}\theta\,\sigma_{nn} - \tfrac{3}{5}P\,V_t^2\right)\\
m_{ttn} &= -\tfrac{m_{nnn}}{2} - \beta\left(\tfrac{1}{14}(R_{tt} + \tfrac{R_{nn}}{2}) + \theta(\sigma_{tt} + \tfrac{\sigma_{nn}}{2}) - P\,V_t^2\right)
\end{aligned} \tag{10}$$

where $\Delta\theta = \theta - \theta_W$, $V_t = v_t - v_t^W$ and

$$P := \rho\,\theta + \frac{\sigma_{nn}}{2} - \frac{R_{nn}}{28\theta} - \frac{R}{120\theta}. \tag{11}$$

The properties of the wall are given by its temperature θ_W and velocity v_t^W and the modified accommodation coefficient

$$\beta = \chi/(2-\chi)\sqrt{2/(\pi\theta)}. \tag{12}$$

In extrapolation of the theory of accommodation these coefficients that occur in every equation of (10) could be chosen differently. This represents a different accommodation of the single moment fluxes, like shear or heat flux, see [30].

The first condition above is the slip condition for the velocity, while the second equation is the jump condition for the temperature. They come in a generalized

form with the essential part given by $\sigma_{tn} \sim V_t$ and $q_n \sim \Delta\theta$. In a manner of speaking, the other conditions can be described as jump conditions for higher moments which again relate fluxes and respective variables. In perfect analogy to the usual slip and jump conditions, the essential part is given by $R_{tn} \sim q_t$ and $m_{nnn} \sim \sigma_{nn}$. The additional terms in 10 are off-diagonal terms coupling all even (in index n) moments in the boundary conditions.

When the R13 equations are considered for channel flows in their original form, it turns out that a different number of boundary conditions is required to solve the fully non-linear and the linearized equations. Since this would not allow a smooth transition between linear and non-linear situations, we formulated the third rule as given above.

Asymptotic analysis shows that some terms can be changed without changing the overall asymptotic accuracy of the R13 equations. This leads to the algebraization of several non-linear terms in the pde's which, after some algebra, leads to algebraic relations, termed as bulk equations, between the moments which serve as additional boundary conditions for the non-linear equations [30],

$$m_{tnn} = \frac{32}{45p}\sigma_{tn}\, q_n \tag{13}$$

$$\hat{R}_{nn} = \frac{136}{25p}q_n^2 - \frac{72}{35\rho}\sigma_{tn}^2, \tag{14}$$

These equations have a special interpretation. The possibility to prescribe kinetic boundary conditions like in (10) for moments is related to the ability of the moments to produce a, so-called Knudsen layer. The Knudsen layer is a boundary layer that occurs close to wall in high Knudsen number flows like in micro channels. The kinetic boundary condition specifies the amplitude of the boundary layer. In the R13-system some variables, like parallel heat flux and normal stresses, are able to produce a Knudsen layer, while others, like the higher moments $\hat{R}_{nn}$ and m_{tnn}, can not. This is due to the finite number of moments considered. In the infinite moment hierarchy all moments exhibit Knudsen layers, see [21].

Due to the lack of a Knudsen layer, kinetic boundary conditions may not be used for the moments $\hat{R}_{nn}$ and m_{tnn}. Instead, we assume that the boundary layer is relaxed infinitely fast to an interior solution - the bulk solution given in (13). Hence, the bulk solution turns out to be the natural boundary conditions for Knudsen-layer-less variables. Details of this interpretation can be found in [30].

4 Achievements with R13

We summarize the most important features of the R13 equations which result from analytical considerations and from analytical and numerical solutions. The results of R13 have been compared to experimental data as well as to direct simulation results obtained by DSMC [3].

The R13 equations:

► are derived in a rational manner by means of the order of magnitude method [22, 24], or from a Chapman-Enskog expansion around non-equilibrium [27, 29], as described above.

► are of third order in the Knudsen number [20, 22, 24, 27, 29], when expanded in a asymptotic expansion and compared to the full expansion of Boltzmann's equation.

► are linearly stable for initial and boundary value problems [27, 29], that is amplitudes of linear sound and heat waves are not amplified.

► contain Burnett and super-Burnett asymptotically in the linear [27] and non-linear [29] case, however, higher order contributions stabilize the R13 system.

► predict phase speeds and damping of sound waves with high frequencies and short wavelengths in excellent agreement to experiments [27].

► give smooth shock structures without subshocks for all Mach numbers, with quantitatively very good agreement to DSMC simulations for $Ma \lesssim 3$ [29].

► are accompanied by a complete set of boundary conditions [30], based on the most commonly used accommodation model in kinetic theory.

► obey an entropy and H-theorem for the linear case, including the boundaries [28], which can also be used to derive the equations as such.

► exhibit the Knudsen paradox, i.e., the minimum of the mass flow rate for channel flows (see next section) [30, 28].

► exhibit Knudsen boundary layers for temperature and velocity profiles as well as other moments in good agreement to DSMC [23, 26].

► are easily accessible to numerical simulations in multiple space dimensions based on finite volume methods [31] or pressure-correction-schemes [9].

► predict dynamic form factors [32] in accordance to experiments of light scattering spectra measuring small scale density fluctuations.

We proceed with presenting the details of micro-channel flows.

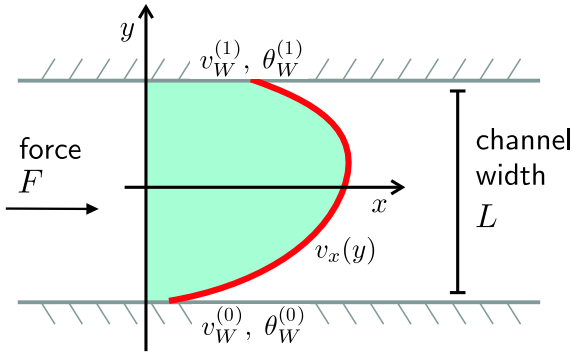

Figure1: General setting for shear fbw between two infi nite plates. The plates are moving and maybe heated.

5 Micro-Channel Flows

To approach micro-channel flows we study a special class of steady shear flows that include steady Couette or Poiseuille flows. For the R13 system, shear flow is a multi-dimensional phenomenon in the sense that it produces a fully multi-dimensional reaction for the stress tensor and heat flux. Introducing $x_i \hat{=} (x, y, z)$, we consider shear flow which is homogeneous in z-direction and define the remaining non-vanishing parts of stress tensor and heat flux as

$$\sigma = \begin{pmatrix} \sigma_{xx} & \sigma_{xy} & 0 \\ \sigma_{yx} & \sigma_{yy} & 0 \\ 0 & 0 & \sigma_{zz} \end{pmatrix}, \quad \mathbf{q} = \left(q_x, q_y, 0\right) \tag{15}$$

where $\sigma_{xy} = \sigma_{yx}$, and $\sigma_{zz} = -(\sigma_{xx} + \sigma_{yy})$ since σ must be trace-free. For the velocity we assume $v_y = v_z = 0$ and

$$\mathbf{v}\,(x, y, z) = (v_x\,(y)\,, 0, 0)\,. \tag{16}$$

The force acts only in x-direction, $\mathbf{f} = (F, 0, 0)$ and enters the momentum balance (2), but no other equation. This setting is valid for channel flows as displayed in Fig. 1. The gas is confined between two infinite plates at distance L and is moving solely in x-direction. The walls are moving with x-velocities $v_W^{(0,1)}$ and may be heated with different temperatures $\theta_W^{(0,1)}$. The Knudsen number

$$Kn = \frac{L}{\lambda} \tag{17}$$

with mean free path $\lambda = \mu/(\rho\sqrt{\theta})$ is based on the width of the channel.

In this setting we have 8 independent variables in the R13 equations, namely $\{\rho, v_x, p, \sigma_{xx}, \sigma_{yy}, \sigma_{xy}, q_x, q_y\}$. Optionally, the pressure p can be replaced by the temperature θ. The 5 remaining relevant constitutive quantities are $\left\{m_{xxy}, m_{xyy}, m_{yyy}, \hat{R}_{xy}, \hat{R}_{yy}\right\}$. The system (1)-(9) reduces to 13 first order non-linear ordinary differential equations in the space variable y. The equations uncover a striking simplicity by decomposing into three linearly decoupled blocks. The coupling is displayed by writing the vector of variables in the form

$$\mathbf{U} = \left\{v_x, \sigma_{xy}, q_x, m_{xyy}, R_{xy} \,|\, \theta, q_y, \sigma_{yy}, \hat{R}_{yy}, m_{yyy} \,|\, \rho, \sigma_{xx}, m_{xxy}\right\} \qquad (18)$$

The first block describes the velocity part with the balances of v_x, σ_{xy}, and q_x, and higher moments m_{xyy} and $\hat{R}_{xy}$, the second block describes the temperature part with balances of θ, q_y, and σ_{yy}, and higher moments $\hat{R}_{yy}$ and m_{yyy}. Both parts are governed dominantly by two classical variables, (v_x, σ_{xy}) and (θ, q_y), respectively, which behave essentially in an intuitive way. In NSF the second variable is related to the gradient of the first. The third variable in both parts, q_x and σ_{yy}, respectively, is given by a seemingly classical variable which however plays a non-intuitive role. It represents a *heat flux produced by a velocity shear* in the first block and a *normal stress due to temperature difference* in the second. Both are typical bulk effects in micro-flows of gases. Through these variables the classical variables velocity and temperature are coupled to the high order internal quantities, m_{xyy} and $\hat{R}_{xy}$, and, $\hat{R}_{yy}$ and m_{yyy}, respectively. From tensorial considerations the first block can be identified with mixed normal/tangential variables (shear), while the second block couples the purely normal variables (temperature). The last block combines the density and purely tangential tensorial variables and exhibits only a minor influence.

5.1 Linear Equations and Knudsen Layers

One of the most important advantages of continuum models is the possibility to gain understanding in micro-gas dynamics through analytical expressions. The mathematical structure of the equations provide a general insight into new physics and may teach intuition about complex processes.

Here, we demonstrate the rise of Knudsen layers and micro-scale variables like non-gradient heat fluxes and normal stresses. Similar calculations can be found in [23, 26].

5.1.1 Velocity Part

As mentioned above the equations split into a velocity and a temperature part in the linear case. The velocity part is governed by the momentum balance and

an equation for shear stress which are given by (2) with force term and the xy-component of (4) and read

$$\partial_y \sigma_{xy} = \rho F \tag{19}$$

$$\sigma_{xy} = -\mu\, \partial_y v_x - \frac{2}{5}\frac{\mu}{p}\partial_y q_x \tag{20}$$

with constant density, pressure and viscosity μ. Obviously, shear stress is given by the velocity gradient, but also by a micro-scale contribution from the heat flux q_x parallel to the walls. This heat flux satisfies the equation (5)

$$\frac{\mu}{\rho}\,\partial_y \sigma_{xy} + \frac{1}{2}\frac{\mu}{p}\partial_y R_{xy} = -\frac{2}{3} q_x \tag{21}$$

$$R_{xy} = -\frac{12}{5}\frac{\mu}{\rho}\,\partial_y q_x \tag{22}$$

with higher order flux R_{xy} given by (7). In particular, the parallel heat flux is independent of a temperature gradient. It is triggered from the shear stress and boundary conditions. Elimination of R_{xy} leads to a second order ordinary differential equation for q_x with solution (assuming symmetry)

$$q_x(y) = -\frac{3}{2}\mu F + C_1 \sinh\left(\frac{1}{Kn}\frac{y}{L/2}\right) \tag{23}$$

using the special Knudsen number $Kn = \frac{3\mu\sqrt{\theta}}{\sqrt{5}\rho L}$. The hyperbolic sine function has the shape of a boundary layer as can be seen in Fig. 2. This boundary layer is superimposed on a bulk solution $\sim \mu F$ in q_x. Finally, the parallel heat flux enters the velocity solution (assuming symmetry)

$$v_x(y) = C_2 + \frac{\rho F}{2\mu}\left((\frac{L}{2})^2 - y^2\right) - \frac{2}{5p} q_x(y) \tag{24}$$

inheriting the Knudsen layer. Hence, the velocity consists of a bulk solution given by the classical parabolic profile and a layer contribution from the parallel heat flux.

Note, that the boundary layers grow quickly with Knudsen number and fill out the channel already at $Kn = 0.5$, see 2. At these Knudsen numbers the bulk and layer in (24) can not be distinguished anymore and the solution will show a quality in its own right with no resemblance to classical solutions.

5.1.2 Temperature part

Remarkably, the temperature part of the linear R13 equations shows identical mathematical structure. The two basic equations are now given by the energy

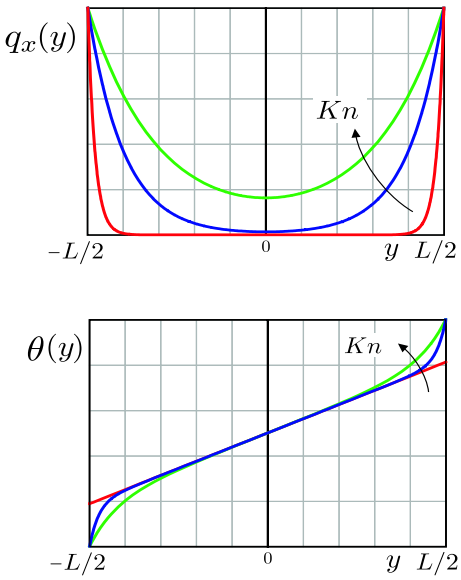

Figure2: R13 predicts exponential Knudsen layers for, e.g., parallel heat flux. The upper plot shows a schematic picture for $F = 0$, $Kn = 0.01, 0.1, 0.5$. These functions lead to typical s-shaped profiles for, e.g., temperature, see the schematic lower plot with $Kn = 0.01, 0.1, 0.2$.

balance (3) and the equation for normal heat flux q_y (5) which read together

$$\partial_y q_y = 0 \tag{25}$$

$$q_y = -\kappa\, \partial_y \theta - \frac{2}{5}\frac{\kappa}{\rho}\partial_y \sigma_{yy} \tag{26}$$

with constant density, pressure and heat conductivity $\kappa = \frac{15}{4}\mu$ (temperature in energy units). Again, the first term on the right hand side describes Fourier's law, but the second shows the influence of normal stress σ_{yy} as a micro-scale variable. This normal stress is determined by the equation (4)

$$\frac{\kappa}{p}\,\partial_y q_y + \frac{2}{9}\frac{\kappa}{p}\partial_y m_{yyy} = -\frac{5}{6}\sigma_{yy} \tag{27}$$

$$m_{yyy} = -\frac{8}{25}\frac{\kappa}{\rho}\,\partial_y q_x \tag{28}$$

with higher order flux m_{yyy} given by relation (7). Note, the perfect analogy to the equations of the velocity part above. Consequently, the normal stress is given by a hyperbolic sine function (assuming anti-symmetry)

$$\sigma_{yy}(y) = C_3 \sinh\left(\frac{1}{Kn}\frac{y}{L/2}\right) \tag{29}$$

exhibiting boundary layer character with a specialized Knudsen number $Kn = \frac{4}{15}\sqrt{\frac{6}{5}}\frac{\kappa\sqrt{\theta}}{\rho L}$. This boundary layer enters the profile of the temperature

$$\theta(y) = C_4 + \frac{C_5}{\kappa}\frac{y}{L/2} - \frac{2}{5p}\sigma_{yy}(y) \tag{30}$$

and leads to typical s-shape as seen in Fig. 2. The bulk solution of σ_{yy} is zero, while the bulk solution of the temperature is the classical linear function.

The integration constants C_i have to be fixed by boundary conditions as given in (10). Similarly to the equations, the boundary conditions also decouple into a velocity and temperature part when linearized.

5.2 Knudsen Paradox

Gas flow through a channel is known to exhibit a paradoxical behavior known as Knudsen paradox, [11].When reducing the Knudsen number in the experiment the normalized mass flow rate

$$J = \int_{-1/2}^{1/2} v(y)\, dy \tag{31}$$

through the channel reaches a minimum and afterwards starts to increase for larger Knudsen numbers.

To model this, we consider Poiseuille flow given by acceleration-driven channel flow with walls at rest and identical temperatures. The channel is considered to be infinitely long such that a steady velocity profile has developed from the viscous boundary layers. The given acceleration can be interpreted as a homogeneous pressure gradient.

Given the analytical result for channel flow of the linear R13-system above it is easy to determine an explicit function for the mass flow rate. After integration we find

$$J = \frac{\gamma_1}{Kn} + \gamma_2\, Kn + \gamma_3$$

where $\gamma_{1,2,3}$ depend on the coefficients in the equations and boundary conditions, like viscosity and accommodation factor. The functional dependence on the Knudsen number is a valuable information. In general, the coefficients could also be calibrated to measurements.

Fig. 3 shows the dimensionless mass flow rate obtained from R13 as a function of Kn. The curve clearly shows a minimum and thus correctly predicts a Knudsen paradox. The figure also shows the mass flow rate obtained with NSF and standard slip boundary conditions which clearly fails to produce a Knudsen minimum. In [19] the mass flow rate has been calculated based on the linearized Boltzmann

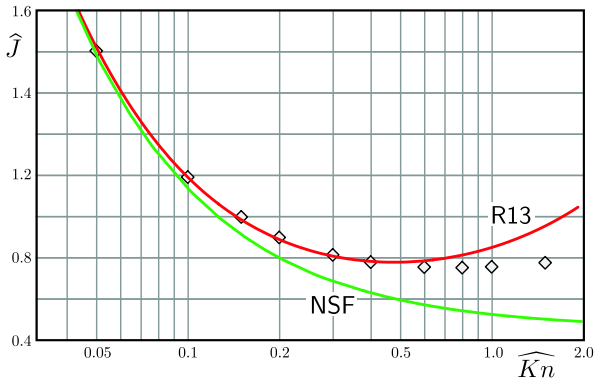

Figure 3: Averaged mass flow rate in acceleration-driven channel flow. The R13-equations predict the Knudsen paradox.

equation and those results are given in Fig. 3 as symbols. The mass flow for R13 follows the Boltzmann result fairly accurate until $Kn \lesssim 1.0$ and then lifts off too quickly. At these high Knudsen numbers the assumptions of the theory are not valid anymore.

Intuitively one would expect a decreasing mass flow for a smaller channel. The explanation for the minimum is the following: For very small Knudsen numbers, viscosity is almost vanishing and a fully developed flow would exhibit a huge velocity profile, hence a very large mass flow rate. When viscosity is increased this profile shrinks, however in the other extreme of large Knudsen numbers a different effect takes over. The interaction between the particles and with the wall becomes so small due to lack of collisions, that the particles are merely accelerated and falling through the channel. Again, a fully developed flow of "accelerated free falling" particles leads to an infinite mass flux. Between these to extrema there must be a minimum. In summary, at a certain micro-scale the friction inside the gas becomes small and the growing slip velocity at the wall dominates the mass flow rate.

5.3 Full Solution

In the linear setting the dissipation term in the energy balance is neglected and any velocity profile does not lead to a temperature rise. To see the temperature profile the non-linear equations have to be solved. Apart from arithmetic complexity this is not a problem with the R13 model.

We solve the full non-linear R13-system in the form (1)-(9) for a Poiseuille flow as described above with kinetic boundary conditions (10)/(13) for various Knudsen numbers.

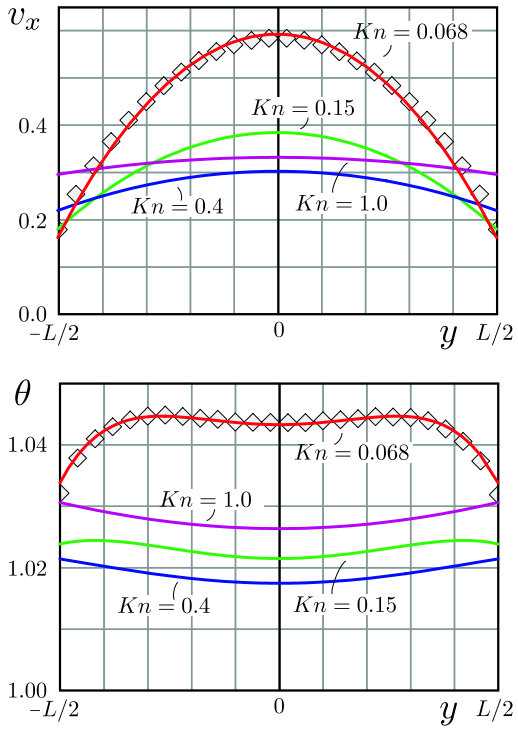

Figure4: Velocity and temperature profi les in acceleration driven channel fbw for various Knudsen numbers. The symbols in the case $Kn = 0.068$ represent a DSMC result.

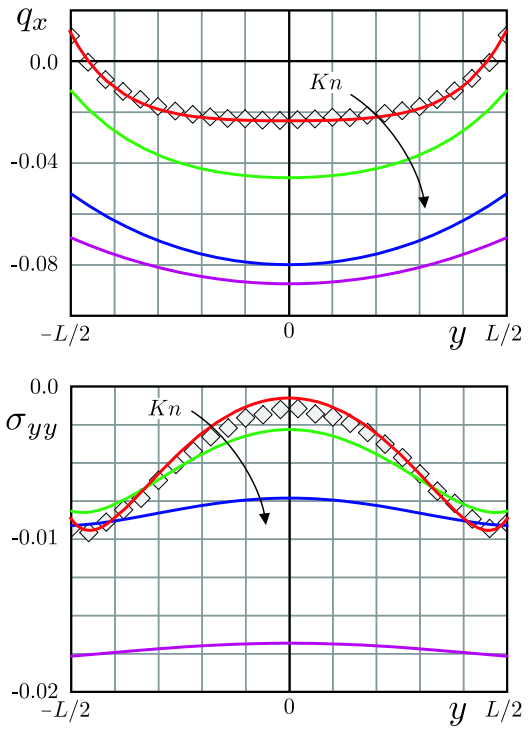

Figure5: Micro-scale effects, like parallel heat flux q_x and normal stresses σ_{yy}, in micro-channels as predicted by R13 for various Knudsen numbers. The symbols in the case $Kn = 0.068$ represent a DSMC result.

The mass flow rate is only a rough property of micro flows and the R13 result gives much more inside when considering the fields of the moments. Figs. 4 and 5 display some fields obtained by R13 for Knudsen numbers $Kn = 0.068,\ 0.15,\ 0.4,\ 1.0$. The figures show the conservation variables velocity v_x and temperature θ, as well as the micro-scale variables tangential heat flux q_x and normal stress σ_{yy}. Note, that the channel flow produces a significant parallel heat flux q_x even though the temperature is homogeneous along x. Similarly, the temperature field triggers a normal stress even though $\partial_y v_y = 0$. This is a micro-scale effect. Higher Knudsen numbers show stronger non-equilibrium as indicated by larger magnitudes of q_x and σ_{yy}. Interestingly, the temperature profile starts to invert for higher Knudsen numbers. Note also, that the Knudsen paradox can be observed in the results of the R13-system in Fig. 4. The velocity profile becomes flatter, but the slip increases and the velocity curve for $Kn = 1.0$ lies above the curve of $Kn = 0.4$.

The simulations were obtained with a dimensionless acceleration force fixed at $F = 0.23$, such that Knudsen number $Kn = 0.068$ corresponds to the case of Poiseuille flow calculated in [35] (see also [33]) by DSMC. These results are shown in Figs. 4 and 5 as symbols. R13 gives good agreement with the DSMC result.

6 Conclusions

With these properties and features, the R13 equations must be considered as the most successful continuum model for gas micro-flows. In contrast to direct simulations or molecular dynamics, such a model gives valuable inside into physical effects by identifying effects inside equations. The application of the R13 equations to a wider variety of micro-flow problems is planned for the future.

Interesting problems to simulate with R13 are thermal creep phenomena like in Knudsen pumps. Also, micro-cavity flows like in [15] are important applications. Challenges are extensions to mixtures and real gases.

Acknowledgement: HS: Support by the Natural Sciences and Engineering Research Council (NSERC) is gratefully acknowledged. MT: Support through the EURYI award of the European Science Foundation (ESF) is gratefully acknowledged.

References

[1] R. K. Agarwal, K. Y. Yun, and R. Balakrishnan, *Beyond Navier-Stokes: Burnett equations for flows in the continuum-transition regime,* Phys. Fluids **13**, (2001), p.3061-3085, Erratum: Phys. Fluids **14**, (2002), p.1818

[2] J. D. Au, M. Torrilhon, and W. Weiss, *The Shock Tube Study in Extended Thermodynamics*, Phys. Fluids **13**(8) , (2001) p.2423-2432

[3] G. A. Bird, *Molecular Gas Dynamics and the Direct Simulation of Gas Flows* (2nd edn), Oxford University Press, New York (1998)

[4] A.V. Bobylev, *The Chapman-Enskog and Grad methods for solving the Boltzmann equation*, Sov. Phys. Dokl. **27**, (1982) p.29-31

[5] A. V. Bobylev, *Instabilities in the Chapman-Enskog Expansion and Hyperbolic Burnett Equations*, J. Stat. Phys. **124** (2-4), (2006), p.371-399

[6] C. Cercignani, *The Boltzmann Equation and its Applications*, Applied Mathematical Sciences 67, Springer, New York, (1988)

[7] B.-C. Eu, *A Modified Moment Method and Irreversible Thermodynamics*, J. Chemical Phys. **73**(6), (1980) p.2958-2969

[8] H. Grad, *On the Kinetic Theory of Rarefied Gases*, Comm. Pure Appl. Math. **2**, (1949), p.331-407

[9] X. Gu and D. Emerson, *A Computational Strategy for the Regularized 13 Moment Equations with Enhanced Wall-Boundary Conditions*, J. Comput. Phys. 225 (2007) p. 263–283

[10] S. Jin and M. Slemrod, *Regularization of the Burnett equations via relaxation*, J. Stat. Phys. **103** (5-6), (2001) p.1009-1033

[11] M. Knudsen, *Die Gesetze der Molekularströmung und der inneren Reibungsströmung der Gase durch Röhren*, Ann. Phys. **333**, (1909), p.75-130

[12] C. D. Levermore, *Moment closure hierarchies for kinetic theories*, J. Stat. Phys. **83**(5-6), (1996) p.1021-1065

[13] D. A. Lockerby and J. M. Reese, *High-resolution Burnett simulations of micro Couette flow and heat transfer*, J. Comput. Phys. **188**(2), (2003), p.333-347

[14] J. C. Maxwell, *On Stresses in Rarefied Gases Arising From Inequalities of Temperature*, Phil. Trans. Roy. Soc. (London) **170**, (1879), p.231-256

[15] S. Mizzi, X.-J. Gu, D. R. Emerson, R. W. Barber, J. Reese, *Application of a High-Order Macroscopic Approach to Force-Driven Poiseuille Flow in the Slip and Transition Regimes*, 1st Intl. Conference on Micro- and Nano-Heat Transfer, Tainan, Taiwan, 2008, MNHT2008-52203

[16] I. Müller, D. Reitebuch, and W. Weiss, *Extended Thermodynamics - Consistent in Order of Magnitude*, Cont. Mech. Thermodyn. **15**(2), (2003) p.411-425

[17] I. Müller and T. Ruggeri, *Rational Extended Thermodynamics* (2nd edn), Springer Tracts in Natural Philosophy (vol.37), Springer, New York (1998)

[18] R.-S. Myong, *A computational method for Eu's generalized hydrodynamic equations of rarefied and microscale gas dynamics*, J. Comput. Phys. **168**(1), (2001) p.47-72

[19] T. Ohwada, Y. Sone and K. Aoki, *Numerical analysis of the Poiseuille and thermal transpiration flows between two parallel plates on the basis of the Boltzmann equation for hard-sphere molecules*, Phys. Fluids A **1**(12), (1989), p.2042-2049

[20] H. Struchtrup, *Macroscopic Transport Equations for Rarefied Gas Flows*, Interaction of Mechanics and Mathematics, Springer, New York (2005)

[21] H. Struchtrup, *Grad's Moment Equations for Microscale Flows*, 23rd Intl. Symposium on Rarefied Gas Dynamics, AIP Proceedings 663, (2003), p.792-799

[22] H. Struchtrup, *Stable transport equations for rarefied gases at high orders in the Knudsen number*, Phys. Fluids **16**(11), (2004) p.3921-3934

[23] H. Struchtrup, *Failures of the Burnett and Super-Burnett equations in steady state processes*, Cont. Mech. Thermodyn. **17**(1), (2005), p.43-50

[24] H. Struchtrup, *Derivation of 13 moment equations for rarefied gas flow to second order accuracy for arbitrary interaction potentials*, Multiscale Model. Simul. **3**(1), (2005) p.221-243

[25] H. Struchtrup, *Scaling and expansion of moment equations in kinetic theory*, J. Stat. Phys. **125**, (2006), p.565

[26] H. Struchtup and T. Thatcher, *Bulk equations and Knudsen layers for the regularized 13 moment equations*, Cont. Mech. Thermodyn. **19**(3) (2007), p.177-189

[27] H. Struchtrup and M. Torrilhon, *Regularization of Grad's 13-Moment-Equations: Derivation and Linear Analysis*, Phys. Fluids **15**/9, (2003), pp.2668-2680

[28] H. Struchtrup and M. Torrilhon, *H-theorem, regularization, and boundary conditions for linearized 13 moment equations*, Phys. Rev. Letters **99**, (2007) 014502

[29] M. Torrilhon and H. Struchtrup, *Regularized 13-Moment-Equations: Shock Structure Calculations and Comparison to Burnett Models*, J. Fluid Mech. **513**, (2004), pp.171-198

[30] M. Torrilhon and H. Struchtrup, *Boundary Conditions for Regularized 13-Moment-Equations for Micro-Channels*, J. Comput. Phys. 227, (2008), p. 1982–2011

[31] M. Torrilhon, *Two-Dimensional Bulk Microflow Simulations Based on Regularized 13-Moment-Equations*, SIAM Multiscale Model. Simul. **5**(3), 695-728 (2006)

[32] M. Torrilhon, *Regularized 13-Moment-Equations*, 25th Intl. Symposium on Rarefied Gas Dynamics, St. Petersburg, Russia, (2006)

[33] K. Xu and Z.-H. Li, *Microchannel flow in the slip regime: gas-kinetic BGK-Burnett solutions*, J. Fluid Mech. 513, (2004) p.87-110

[34] W. Weiss, *Continuous shock structure in extended Thermodynamics*, Phys. Rev. E **52**, (1995), p.5760

[35] Y. Zheng, A. L. Garcia, and J. B. Alder, *Comparison of kinetic theory and hydrodynamics for Poiseuille flow*, J. Stat. Phys. **109**, (2002), p.495-505